Journal of Materials Chemistry C

High-temperature tolerance of piezoresistive effect in p-4H-SiC for harsh environment sensing

Journal:	*Journal of Materials Chemistry C*
Manuscript ID	TC-COM-06-2018-003094.R1
Article Type:	Communication
Date Submitted by the Author:	15-Jul-2018

Complete List of Authors:	Nguyen, Tuan-Khoa; Griffith University, Queensland Micro and Nano technology centre; Queensland Micro- and Nanotechnology Centre, Phan, Hoang-Phuong; Griffith University, Queensland Micro-Nanotechnology Centre Dinh, Toan; Griffith University, Queensland Micro-Nanotechnology Centre Md Foisal, Abu Riduan; Griffith University, Queensland Micro- and Nanotechnology Centre Nguyen, Nam-Trung; Griffith University, Queensland Micro- and Nanotechnology Centre Dao, Dzung; Griffith School of Engineering, Griffith University

SCHOLARONE™
Manuscripts

Journal Name

ARTICLE TYPE

Cite this: DOI: 10.1039/xxxxxxxxxx

High-temperature tolerance of piezoresistive effect in p-4H-SiC for harsh environment sensing†

Tuan-Khoa Nguyen,*[a] Hoang-Phuong Phan,[a] Toan Dinh,[a] Abu Riduan Md Foisal,[a] Nam-Trung Nguyen,[a] and Dzung Viet Dao,[ab]

Received Date
Accepted Date

DOI: 10.1039/xxxxxxxxxx

www.rsc.org/journalname

4H-silicon carbide based sensors are promising candidate to replace prevalent silicon-based counterparts in harsh environment owing to the superior chemical inertness, high stability and reliability. However, the wafer cost and difficulty in the metallization process to obtain Ohmic contact hinders the use of this SiC polytype in practical sensing applications. This article presents the high-temperature tolerance of a p-type 4H-SiC piezoresistor at elevated temperatures up to 600°C. A good Ohmic contact was formed by the metallisation process using titanium and aluminium annealed at 1000°C. The leakage current at high temperature was measured to be negligible thanks to the robust p-n junction. Owing to superior physical properties of the bulk 4H-SiC material, a high gauge factor of 23 was obtained at 600°C. The piezoresistive effect also exhibits good linearity and high stability at high temperatures. The results demonstrate the capability of p-type 4H-SiC for the development of highly sensitive sensors in hostile environments.

The developments of hostile environment sensors are hindered by the current technologies relying on the silicon (Si) material. For instance, Si experiences plastic deformation at 500°C and instability at high temperature or in corrosive environments. In contrast, the superior tolerance to high temperatures, corrosive media, intensive shock positions silicon carbide (SiC) a promising material for a broad range of applications in hostile environments.[1] Moreover, the progresses of the wafer growth and fabrication process not only cuts down the cost of SiC wafers, but also greatly improves the film quality and reliability of SiC devices. In terms of micro-machining, SiC can inherit the strong foundation and maturity of Si technology infrastructures, which enables the batch production of SiC sensing devices for corrosive or harsh environment sensing. Piezoresistive effect has been considered as the main transduction mechanism for mechanical sensors such as strain/pressure/acceleration sensing, thanks to the simplicity of the read-out circuitries and the wide linearity range.[2,3] When a mechanical stress/strain is applied to a piezoresistive based sensing element, the energy band is significantly modified, leading to the large variation of the electrical conductivity (or the resistivity).[4–6]

Due to the different arrangement of Si and C atoms in the crystal structure, there are more than 200 SiC polytypes which have been discovered. 3C-SiC, 4H-SiC and 6H-SiC are the most common and commercially available polytypes to date. Over the last four decades, many studies have investigated the piezoresistive effect of these polytypes for mechanical sensing applications. Shor *et al.* revealed a gauge factor (GF) of -31.8 for n-type single crystalline 3C-SiC grown on a Si substrate with the doping concentration of 10^{17} cm^{-3}.[7] Phan *et at.* reported GFs of p-type 3C-SiC to be 25 – 28 at temperatures varying from 300°K to 573°K using an *in situ* approach.[3] In α-SiC, the GFs of highly doped (i.e. 2×10^{19} cm^{-3}) n-type and p-type 6H-SiC at room temperature were found to be -22 and 27, respectively; these GFs decreased by half at 250°C.[8] Akiayama *et al.* measured the GF of n-type highly doped 4H-SiC at room temperature to be 20.8 for transverse piezoresistors.[9] Amongst the three most common SiC polytypes, 4H-SiC possesses the highest energy band gap (i.e. 3.26 eV) with a high potential barrier which can effectively minimize the generation of electron-hole pairs by increasing temperatures. This results in the good stability and reliability of 4H-SiC electronics devices in high-temperature operations.[10,11] Additionally, the superior physical properties combined with high

[a] Queensland Micro- and Nanotechnology Centre, Griffith University, Brisbane, Queensland 4111, Australia
[b] School of Engineering and Built Environment, Griffith University, Gold Coast, Queensland 4215, Australia

† Electronic Supplementary Information (ESI) available: [details of any supplementary information available should be included here]. See DOI: 10.1039/b000000x/
‡ Additional footnotes to the title and authors can be included *e.g.* 'Present address:' or 'These authors contributed equally to this work' as above using the symbols: ‡, §, and ¶. Please place the appropriate symbol next to the author's name and include a `\footnotetext` entry in the the correct place in the list.

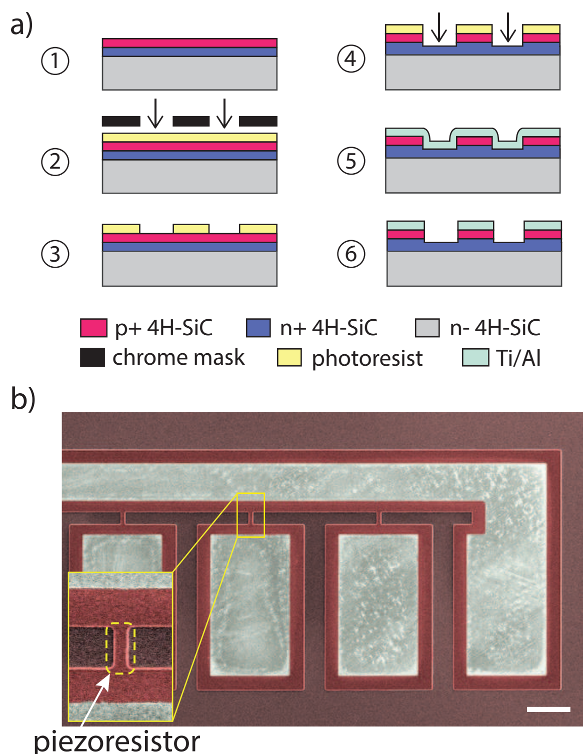

Fig. 1 a) Fabrication process of the 4H-SiC piezoresistors: ① Starting p-on-n 4H-SiC wafer; lithography process including ② UV exposer and ③ photoresist removal; ④ ICP etching of p-type 4H-SiC; ⑤ metal deposition; ⑥ pattern metal contact. b) SEM image of as-fabricated 4H-SiC piezoresistors. Scale bar, 100μm.

break-down voltage makes 4H-SiC the most important SiC polytype for high-power electronics, including Schottky diodes, high power-switching devices, bipolar junction transistors (BJT)[12–14] and metal oxide semiconductor field effect transistors (MOSFET).[10] In terms of sensing devices, to date there are limited studies on the 4H-SiC sensors for high temperature applications due to several challenges. Firstly, the developments of high quality SiC film growth recently enables the availability of p-4H-SiC wafers whereas engineering-graded n-4H-SiC wafers have been available for a decade. Another factor is the difficulty in the formation of the Ohmic contact to p-4H-SiC,[15,16] which limits studies on the piezoresistive effect of p-4H-SiC. Additionally, the deployment of straining configurations which can effectively induce strain to thin-film piezoresistors at high temperature is challenging. These obstacles result in the lack of understanding of the piezoresistive effect of 4H-SiC at elevated temperatures which is solely based on theoretical analyses, such as a first principle simulation in SiC nanosheets[17] and a deformation potential approximation.[18]

In this article, we present the first experimental study on the piezoresistive effect of p-type 4H-SiC at high temperatures up to 600°C. As such, high gauge factors were obtained to be 33 at room temperature and 23 at 600°C. The high sensitivity and good stability at elevated temperatures are attributed to the superior physical properties of 4H-SiC as well as the robust p-n junction which prevents the current from leaking to the substrate. This demonstrated the capability of p-type 4H-SiC for hostile environment sensing where the use of Si or polymer based devices is infeasible.

The p-type 4H-SiC piezoresistive element was fabricated from a bulk 4H-SiC wafer which is commercially available from Cree^{TM}. The wafer consists of an epitaxial highly doped (i.e. carrier density of 10^{18} cm^{-3}) p-type 4H-SiC on the top, n-type 4H-SiC lying in the middle and a low doped n-type substrate. The thickness of either p-type and n-type layers are 1μm while that of the substrate is 350μm. The wafer was cleaned prior to a photolithography process using AZ9245 to form a patterned photoresist mask with a thickness of 4μm for subsequent etching of SiC. The patterned mask SiC wafer was anisotropically etched in a STS SR^{TM} inductive couple plasma (ICP) system for 10 min with 1500W coil power. A 50 sccm HCl flow at a pressure of 2mTorr was supplied. After ICP etching, the remaining photoresist mask was removed by acetone and isopropanol, then thoroughly rinsed in deionized water. The etch depth of 1.3 μm was measured by a Dektak^{TM}150 profiler, ensuring that the unmasked p-type regions were completely removed, as shown in Fig. 1(a). To form the metal contact, 100-nm-thick Ti and Al layers were subsequently sputtered in a SNS^{TM} Sputterer. Another photolithography step was performed to create the contact patterned mask prior to the wet etching of Al and Ti by an Al etchant (i.e. H_3PO_4) and a mixture of hydrogen fluoride (HF) and hydrogen peroxide (H_2O_2), respectively. Subsequently, the wafer was thoroughly rinsed and cleaned by deionized water. After the metallisation, the wafer was annealed by a rapid thermal annealing (RTP) process at 1000°C for 3 min to create the Ohmic contact. Investigations on the Ohmic contact to p-type 4H-SiC have been extensively investigated,[15,16,19] and the Ohmic contact formation of Ti/Al to p-type 4H-SiC annealed at 1000°C occurs in two stages.[16] In the early stage, Ti and Al react to form $TiAl_2$, $TiAl_3$ and Ti_3Al, leaving unre-

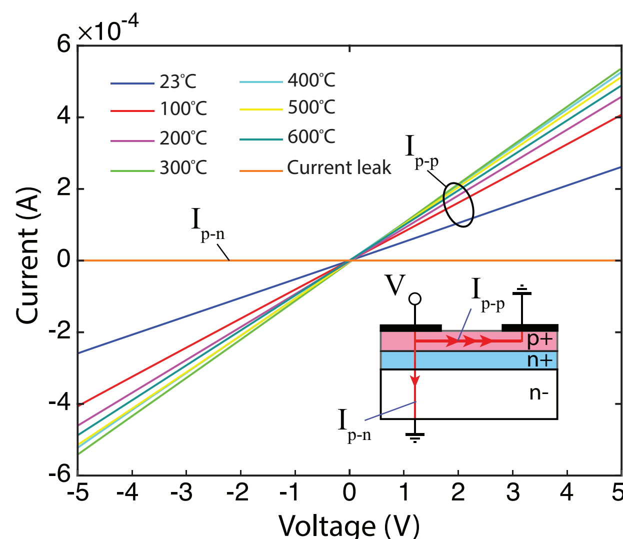

Fig. 2 Current-voltage characteristics of the p-type piezoresistor with a voltage ranging from -5V to 5V at various temperatures from 23°C to 600°C, showing the linear Ohmic characteristics of the Ti/Al contact to the p-type layer. Inset: Schematic sketch of the measurement of the current flowing in p-type layer and through the p-n junction.

This journal is © The Royal Society of Chemistry [year]

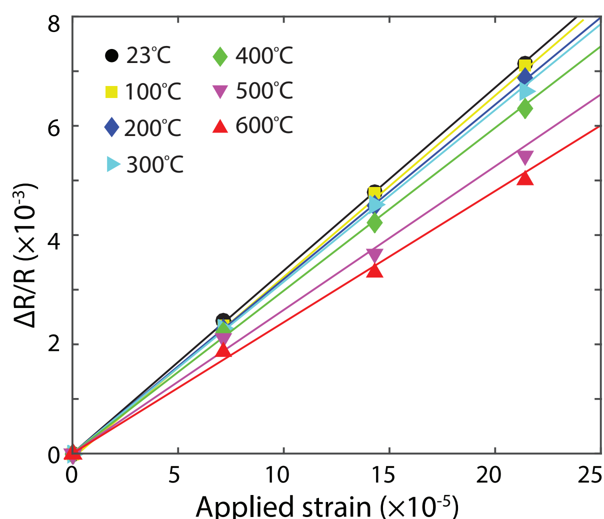

Fig. 3 Fractional change of resistance of the p-type 4H-SiC piezoresistor with various applied strains of up to 215ppm, showing the good linearity of the piezoresistive effect at high temperatures.

acted C atoms at the Ti/SiC interfaces. Subsequently, in the later stage, the reactions of the Ti, SiC and C form a ternary Ti_3SiC_2 compound. The use of thin Al and Ti ensures that all metal layers react into the compounds in the two stages. Subsequently, the reaction of SiC and the contact materials increases the doping concentration in the region close to the SiC/metal interface and forms the Ohmic contact. The contact resistance was measured to be approximately 10^{-3} Ωcm^2 at room temperature then increased about 30% at 600°C. In the final step, the wafer was diced into 30×3 mm^2 beams prior to the piezoresistive effect measurement.

The 4H-SiC beams were placed in a temperature-controlled probe system (i.e. Linkam^{TM}HFS600E-PB2). The temperature of the probe chamber was precisely regulated by a built-in closed-loop control in the temperature controller unit. The upper limit of temperature in this work is restricted by the equipment. The small temperature tolerance (i.e.±0.1°C) minimizes the deviation of the resistance change by the temperature variation. The sensitivity of the 4H-SiC piezoresistor was defined by the fractional change of the resistance versus applied strain as

$$GF = (1+2\upsilon) + \frac{\Delta R/R}{\varepsilon} \quad (1)$$

where ε is the strained induced to the piezoresistor, υ is the Poisson's ratio of 4H-SiC. In SiC material, the first term of Eq. 1 represents the change due to the geometrical effect under strain which is inferior to the second term of the piezoresistive effect. To characterise the piezoresistive effect of 4H-SiC, a uniaxial strain was induced to the piezoresistor using a bending method.[9,28,29] The analytical model is a double-layer cantilever with one clamped end, while a static force was applied to the other end. Subsequently, a uniaxial strain was effectively transferred to the piezoresistor lying on the top surface of the cantilever (see Electronic Supplementary Information for the analysis of the straining model). The bending configuration is depicted in Fig. 4:Inset in which one end of the 4H-SiC beam was fixed on the hot plate by probes while the other end was deflected by a static force.

For Si based devices the p-n junction cannot withstand temperature above 200°C due to the thermally activated electron-hole pairs generation, leading to the instability and reliability in the operation. In contrast, the large energy band gap in 4H-SiC forms a high potential barrier, enabling the stability at high temperatures. We confirmed this property in 4H-SiC by characterizing the rectification behaviour of 4H-SiC p-n junction at elevated temperatures up to 600°C using a Keithley^{TM} 2602. Figure 2 shows the current-voltage characteristics of the p-type piezoresistor and the current leak through the p-n junction at a temperature range from 23°C to 600°C. The measured leakage current was approximately three orders of magnitudes smaller then the current flowing in the p-type sensing layer. For example, at an applied voltage of 5V at 600°C, the current in the p-type was approximately 460μA while the leakage current was measured below 1nA. This is attributed to the robust back-to-back p/n diode preventing the current from leaking to the substrate.[9,30] The very small current leaking to the substrate demonstrates a significant advantages of 4H-SiC over other low band gap materials for mechanical sensing at elevated temperatures.

The relative resistance change versus applied strain ranging from 0 to 215ppm at temperatures from 23°C to 600°C was illustrate in Fig. 3. Evidently, the p-type 4H-SiC piezoresistors exhibited an good linearity in the chosen strain range. The measured GF at a varying temperature were shown in Fig. 4. The GF at room temperature was approximately 33, then gradually decreased to about 23 at 600°C. This is equivalent to a reduction of sensitivity of approximately 30% at the given temperature range. The result agrees well with the decrease trend of the GF with the increase of the ambient temperatures in other reports for SiC polytypes (Table 1). It should be noted that, p-type 4H-SiC is able to retain the relatively high GF at 600°C, which is ten times higher than the GF of conventional metal strain gauges at room temperature. When the temperature increases, the ioniza-

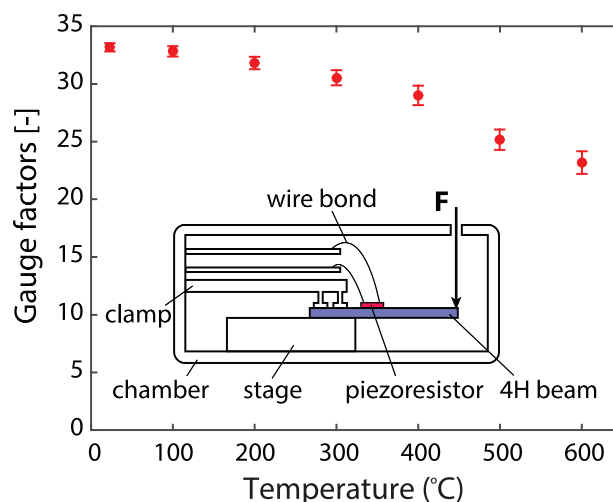

Fig. 4 Measured gauge factor of p-type 4H-SiC at a temperature ranging from 23°C to 600°C; the GF at 600°C decreases about 30% in comparison with the GF at room temperature. Inset: Schematic sketch of the bending beam experiment in a Linkam^{TM} chamber (not to scale).

Table 1 Comparison of the gauge factor in various SiC polytypes at high temperature

Material	Carrier type	Doping concentration (cm^{-3})	Maximum temperature	Gauge factor (room temp.→max temp.)
3C-Si[20]	N	2.9×10^{18}	573K	-32 → -14
3C-SiC[7]	N	10^{16}-10^{17}	450°C	-31.8 → -17
3C-SiC[21]	N	unintentionally	400°C	-18 → -7
3C-SiC[22]	N	10^{19}	400°C	-24 → -11
3C-SiC[23]	N	-	400°C	-16 → -12.5
3C-SiC[24]	N	-	200°C	-18 → -10
3C-SiC[25]	P	-	300°C	28 → 25
6H-SiC[26]	N	1.8×10^{17}-3×10^{18}	250°C	-29.4 → -17
6H-SiC[8]	N	2×10^{19}	250°C	-22 → -11.5
	P	2×10^{19}	250°C	27 → 11.5
Poly-SiC[27]	N	10^{18}-10^{20}	200°C	10 → 7
4H-SiC (this work)	P	10^{18}	600°C	33 → 23

tion effect raises the carrier concentration as well as the electrical conductance of p-type 4H-SiC (Fig. 2). As a consequence, the increases in the carrier concentration and the carrier scattering will reduce the GF in p-type 4H-SiC. This hypothesis was confirmed by the experimental results, as shown in Fig. 3 and 4. However, the GF did not significantly decrease in the wide range of temperature. This result is attributed to the high carrier concentration of the p+ layer used in this work, which stabilized the Fermi-Dirac integral at high temperature and resulted in the relatively stable GF.

The GFs of different SiC polytypes including 3C-, 6H-, 4H-SiC at high temperatures, was summarised in Table 1. There are a number of factors for the variation in the GF amongst different studies, including the differences in the SiC polytypes, the impurity concentrations, and the quality/growth processes of SiC films. The dopant type (n or p) typically dictates the sign of the GFs (i.e. "-" sign for longitudinal n-type or transverse p-type piezoresistors and "+" sign for transverse n-type or longitudinal p-type piezoresistors). Moreover, the GF normally decreases with increasing the carrier concentration and with increasing temperature.[31] The positive (or negative) values of the GF indicate the conductivity of the SiC piezoresistors decrease (or increase) with increasing stress/strain. In terms of sensing devices, only the magnitude of the GF is significant not the sign. However, in the case of mobility enhancement, it is possible to significantly increase the electron mobility in p-type/n-type SiC by utilizing the transverse/longitudinal strains (with negative GF). Akiyama *et.al* reported the GF of n-type 4H-SiC with the highest value of 20.8 for transverse resistors and -10 for longitudinal resistors at room temperature. In comparison, our measured GF for p-type 4H-SiC are significantly higher (i.e. 33 at room temperature and 23 at 600°C). This means that the use of p-type 4H-SiC will yield a higher sensitivity over the n-type counterpart. Additionally, the as-fabricated p-type 4H-SiC piezoresistor are able to retain a relatively high GF at elevated temperatures where the use of other common semiconductors (e.g. silicon, polymers) is not possible.

The variation of the electrical conductivity of p-type 4H-SiC is due to the increased ionization effect by temperature. Under strain, there is the hole transfer between the top valence bands including the light hole (LH), heavy hole (HH), and spin-orbit split-off (SOSO) bands. In the energy band of 4H-SiC, the band gaps between the light hole band versus the heavy hole and SOSO bands are 0.15eV and 0.65eV, respectively.[32] Additionally, the hole concentration ratio between valence bands is $e^{\Delta E/k_BT}$. Substituting the Boltzmann constant k_B=1.38 $\times10^{-23}$ JK^{-1} and the temperature range T=298 – 873K, we derive p_1/p_2 = 7.3 – 300 and p_1/p_{SOSO} = 5.6×10^3 – 9.7×10^{10}, where p_1, p_2, and p_{SOSO} are the hole concentrations of the LH, HH, and SOSO bands, respectively. This means that the number of holes occupied in the LH band is much larger than that in the HH and SOSO bands and the majority of the holes are located in the LH band, leading to the dominant effect of the LH band over the HH and SOSO bands in the piezoresistivity of p-type 4H-SiC. Therefore, the change of electrical conductivity of p-type 4H-SiC can be considered solely dependent on the redistribution of the holes in the LH band under strain and the ambient temperature T as[33]

$$\frac{\Delta\sigma}{\sigma} \sim \frac{\Delta p_1}{p_1} = \frac{1}{k_BT}\frac{\Delta E_V}{1+(m_1^*/m_2^*)^{3/2}} \quad (2)$$

where m_1^* and m_2^* are the effective masses of the hole in the LH and HH bands, respectively; ΔE_V is the band splitting energy as a function of the induced stress to the crystal lattice. From Eq. 2, it can be realized that the relative resistance change (or conductivity variation) is almost inversely proportional to the increase of the ambient temperature, which is in good agreement with the experimental data (Fig. 4).

In conclusion, high gauge factor of p-type 4H-SiC were obtained with a good linearity and stability at high temperatures up to 600°C. At 600°C the gauge factor was found to be approximately 23 which is at least ten times higher than the conventional metal strain gauges. The measured piezoresistivity of p-type 4H-SiC with temperature is in good agreement with the hole transfer model in p-type SiC. The high gauge factor of p-type 4H-SiC demonstrates the potential for mechanical sensing in hostile environments where the use of Si or polymer counterparts is infeasible.

Acknowledgement

This work has been partially supported by Australian Research Council grants LP150100153 and LP160101553. This work was also supported by the Queensland node of the Australian National Fabrication Facility, a company established under the National Collaborative Research Infrastructure Strategy to provide nano and micro-fabrication facilities for Australian researchers.

 This journal is © The Royal Society of Chemistry [year]

Conflicts of interest

There are no conflicts to declare.

Notes and references

1 Z. He, L. Wang, F. Gao, G. Wei, J. Zheng, X. Cheng, B. Tang and W. Yang, *CrystEngComm*, 2013, **15**, 2354.
2 T.-K. Nguyen, H.-P. Phan, J. Han, T. Dinh, A. R. M. Foisal, S. Dimitrijev, Y. Zhu, N.-T. Nguyen and D. V. Dao, *RSC Adv.*, 2018, **8**, 3009–3013.
3 H.-P. Phan, T. Dinh, T. Kozeki, T.-K. Nguyen, A. Qamar, T. Namazu, N.-T. Nguyen and D. V. Dao, *IEEE Electron Device Lett.*, 2016, **37**, 1029.
4 J. Bi, G. Wei, L. Wang, F. Gao, J. Zheng, B. Tang and W. Yang, *J. Mater. Chem. C*, 2013, **1**, 4514.
5 F. Gao, J. Zheng, M. Wang, G. Wei and W. Yang, *Chem. Commun.*, 2011, **47**, 11993.
6 X. Li, S. Chen, P. Ying, F. Gao, Q. Liu, M. Shang and W. Yang, *J. Mater. Chem. C*, 2016, **4**, 6466–6472.
7 J. Shor, D. Goldstein and A. Kurtz, *IEEE Trans. Electron Devices*, 1993, **40**, 1093–1099.
8 R. Okojie, A. Ned, A. Kurtz and W. Carr, *IEEE Trans. Electron Devices*, 1998, **45**, 785.
9 T. Akiyama, D. Briand and N. F. de Rooij, *J. Micromech. Microeng.*, 2012, **22**, 085034.
10 N. G. Wright, A. B. Horsfall and K. Vassilevski, *Mater. Today*, 2008, **11**, 16–21.
11 B. J. Baliga, *Silicon carbide power devices*, World scientific, 2006.
12 L. Lanni, R. Ghandi, B. G. Malm, C.-M. Zetterling and M. Ostling, *IEEE Trans. Electron Devices*, 2012, **59**, 1076–1083.
13 S. Singh and J. A. Cooper, *IEEE Trans. Electron Devices*, 2011, **58**, 1084–1090.
14 A. Siddiqui, H. Elgabra and S. Singh, *J. Electron Devices Soc.*, 2018, **6**, 126–134.
15 L. Fursin, J. Zhao and M. Weiner, *Electronics Letters*, 2001, **37**, 1092.
16 R. Konishi, R. Yasukochi, O. Nakatsuka, Y. Koide, M. Moriyama and M. Murakami, *Mat. Sci. Eng.: B*, 2003, **98**, 286–293.
17 K. Nakamura, T. Toriyama and S. Sugiyama, *Japanese J. Appl. Phys.*, 2011, **50**, 06GE05.
18 T. Toriyama, *J. Micromech. Microeng.*, 2004, **14**, 1445–1448.
19 H. Vang, M. Lazar, P. Brosselard, C. Raynaud, P. Cremillieu, J.-L. Leclercq, J.-M. Bluet, S. Scharnholz and D. Planson, *Superlattices Microstruct.*, 2006, **40**, 626–631.
20 R. Ziermann, J. von Berg, W. Reichert, E. Obermeier, M. Eickhoff and G. Krotz, Proc. Inter. Solid State Sens. Act. Conf. (Transducers), 1997.
21 C.-H. Wu, C. Zorman and M. Mehregany, *IEEE Sensors J.*, 2006, **6**, 316–324.
22 M. Eickhoff and M. Stutzmann, *J. Appl. Phys.*, 2004, **96**, 2878–2888.
23 J. Strass, M. Eickhoff and G. Kroetz, Proc. Inter. Solid State Sens. Act. Conf. (Transducers), 1997.
24 M. Eickhoff, H. Möller, G. Kroetz, J. v. Berg and R. Ziermann, *Sens. Actuators, A*, 1999, **74**, 56–59.
25 H.-P. Phan, T. Dinh, T. Kozeki, A. Qamar, T. Namazu, S. Dimitrijev, N.-T. Nguyen and D. V. Dao, *Sci. Rep.*, 2016, **6**, 28499.
26 J. Shor, L. Bemis and A. Kurtz, *IEEE Trans. Electron Devices*, 1994, **41**, 661–665.
27 T. Homma, K. Kamimura, H. Y. Cai and Y. Onuma, *Sens. Actuators, A*, 1994, **40**, 93–96.
28 H.-P. Phan, T. Dinh, T. Kozeki, T.-K. Nguyen, A. Qamar, T. Namazu, N.-T. Nguyen and D. V. Dao, *Appl. Phys. Lett.*, 2016, **109**, 123502.
29 T.-K. Nguyen, H.-P. Phan, T. Dinh, J. Han, S. Dimitrijev, P. Tanner, A. R. M. Foisal, Y. Zhu, N.-T. Nguyen and D. V. Dao, *IEEE Electron Device Lett.*, 2017, **38**, 955–958.
30 T.-K. Nguyen, H.-P. Phan, T. Dinh, T. Toriyama, K. Nakamura, A. R. M. Foisal, N.-T. Nguyen and D. V. Dao, *Applied Physics Letters*, 2018, **113**, 012104.
31 T. Toriyama and S. Sugiyama, *J. Microelectromech. Syst.*, 2002, **11**, 598–604.
32 C. Persson and U. Lindefelt, *J. Appl. Phys.*, 1997, **82**, 5496–5508.
33 P. Kleimann, B. Semmache, M. L. Berre and D. Barbier, *Phys. Rev. B*, 1998, **57**, 8966.

This journal is © The Royal Society of Chemistry [year]